

RELATIVISTICALLY PARAMETERIZED EXTENDED HÜCKEL CALCULATIONS

VI *. INTERPRETATION OF NUCLEAR SPIN—SPIN COUPLING CONSTANTS IN SOME ORGANOLEAD COMPOUNDS

P. PYYKKÖ

Department of Physical Chemistry, Åbo Akademi, SF - 20500 Åbo (Turku) (Finland)

(Received January 13th, 1982)

Summary

Relativistically parameterized extended Hückel (REX) molecular orbitals and the relativistic analogue of Ramsey's theory are used to calculate ${}^1K(\text{MC})$ and ${}^1K(\text{MM})$ coupling tensors in the model systems HCCPbH_3 and Pb_2H_6 as well as in $\text{M}(\text{CCH})_4$ ($\text{M} = \text{Sn}, \text{Pb}$) and $\text{Pb}_2(\text{CH}_3)_6$. The s AO or "contact" contribution dominates the coupling. The large variations of these coupling constants as functions of chemical substitution are ascribed to changes of the mutual polarisability π , due to the presence of a node surface near the Pb nucleus in the highest occupied σ MO. This "frontier MO" dominates the coupling because of a relativistic isolation of most of the Pb $6s$ character in deeper MOs.

1. General

1.1. Experimental background

The one-bond ${}^1K(\text{MM})$ and ${}^1K(\text{MC})$ ($\text{M} = \text{Sn}, \text{Pb}$) spin—spin coupling constants show several features which have evaded a simple explanation. Although the ratio of the valence s hyperfine integrals is $\nu_{-1}(\text{Pb})/\nu_{-1}(\text{Sn}) = 3.374$ (non-relativistically 1.562) [1], the ratio of the coupling constants, ${}^1K(\text{Pb})/{}^1K(\text{Sn})$ may vary widely, between 0.61 and 1.49 [2] or between -233 and 2.73 [3]. The ${}^1K(\text{SnSn})$ are sensitive to substituents [4] and may in fact, become negative [5]. Both the ${}^1K(\text{PbC})$ [6] and the ${}^1K(\text{PbPb})$ [7] of Pb_2Me_6 are very small and, in $\text{HC}\equiv\text{C}-\text{MR}_3$, the ${}^1K(\text{MC})$ is very sensitive to the substituent R, becoming negative for $\text{M} = \text{Pb}$ and $\text{R} = \text{Et}$ [8].

* References 12, 14, 1 and 15 form parts I, III, IV and V of the present series.

1.2. Earlier theoretical discussions

Starting from Ramsey's non-relativistic theory of spin-spin coupling [9a], keeping only the Fermi-contact term and introducing an MO-LCAO approximation with one centre matrix elements only, the reduced spin-spin coupling constant between nuclei A and B becomes (in SI units) [9b]:

$$K(AB) = \frac{4}{9} \mu_0^2 \beta^2 \psi_A(0)^2 \psi_B(0)^2 \pi_{AB} (\text{m}^{-2} \text{kg s}^{-2} \text{A}^{-2}) \quad (1)$$

with the mutual polarisability:

$$\pi_{AB} = 4 \sum_i^{\text{occ}} \sum_j^{\text{unocc}} c_{iA} c_{jA} c_{jB} c_{iB} / (E_i - E_j) \quad (2)$$

Introducing for all excitations $i \rightarrow j$ the same energy denominator ΔE and using the closure

$$\sum_i |i\rangle \langle i| = 1, \quad (3)$$

eq. 1 reduces to

$$K(AB) = \frac{4}{9} \mu_0^2 \beta^2 \psi_A(0)^2 \psi_B(0)^2 \alpha_A^2 \alpha_B^2 / |\Delta E|, \quad (4)$$

where α_A^2 is the s character of atom A.

As the variations in ΔE , $\psi(0)^2$ or the s characters of eq. 4 cannot possibly be large enough to explain the observed variations of 1K , the use of eq. 1 has been proposed [3,5]. In a simple case like the ${}^1K(\text{SnX})$ of the pyramidal SnX_3^- the cancellation of the positive $1a_1 \rightarrow 3a_1$ contribution against a negative $2a_1 \rightarrow 3a_1$ one, $2a_1$ being the lone pair orbital, can be invoked to explain the small or negative values [1,5a,10]. No other discussions on the nature of the relevant MOs i and j in the present compounds are known to us. The object of this work is to use the relativistic analogue of Ramsey's theory [11] and "Relativistically parameterized Extended Hückel (REX)" MOs [1,12-15] to find somewhat more detailed explanations for the observations in §1.1.

2. Theory

2.1. The REX method

This non-iterative method consists of a single diagonalization of a Hamiltonian matrix, set up using $|lsjm_j\rangle$ basis orbitals on each atom, thus doubling the usual EHT basis size. The diagonal matrix elements h_{ii} are set equal to calculated relativistic Hartree-Fock orbital energies in the neutral atoms. The off-diagonal elements are obtained from the Wolfsberg-Helmholz formula. The orbital exponents of the Slater orbitals are obtained from a fit to the atomic radial functions, as described in ref. 14. The REX program [13] contains default parameters for the elements 1-120. The program requires only the molecular geometry and yields molecular orbitals permitting a systematic comparison of the relativistic and non-relativistic cases at the EHT level of cost and performance.

Examples of the importance of relativistic effects in heavy-atom chemistry are given in reviews [16-18].

2.2. The relativistic theory of nuclear spin—spin coupling

For heavy elements Ramsey's theory [9a] becomes inaccurate both because the hyperfine Hamiltonian used is entirely non-relativistic and because LS-coupling is assumed for the electronic wave functions. In its relativistic counterpart [11] the relativistic hyperfine Hamiltonian

$$\mathcal{H} = eca \cdot A \quad (5)$$

and jj -coupled wave functions are used, α being a Dirac matrix and A the magnetic vector potential of the nuclei. Writing the spin—spin coupling energy between nuclei A and B as

$$\mathcal{H} = g_A g_B \beta_n^2 \sum_{\mu, \nu = -1}^1 I_{A\mu} K_{AB}^{\mu\nu} I_{B\nu} \quad (6)$$

and including one-centre matrix elements only, the reduced coupling tensor becomes

$$\zeta_{AB}^{\mu\nu} = 2 \sum_i^{\text{occ}} \sum_j^{\text{unocc}} \left(\sum_{t, \mu \in A} c_{it}^* c_{j\mu} \langle \chi_t | (V_A^\mu)^\dagger | \chi_\mu \rangle \right) \times \left(\sum_{v, w \in B} c_{jv}^* c_{iw} \langle \chi_v | (V_B^\nu)^\dagger | \chi_w \rangle \right) (E_i - E_j)^{-1}. \quad (7)$$

Here the matrix elements between the atomic orbitals χ become

$$c_{it} m_t | (V_A^\mu)^\dagger | c_{j\mu} m_\mu = ec(\mu_0/4\pi) (-1)^{l_t + j_t - m_\mu} \times (2(2j_t + 1)(2j_\mu + 1))^{1/2} \begin{pmatrix} j_t & 1 & j_\mu \\ \frac{1}{2} & -1 & \frac{1}{2} \end{pmatrix} \begin{pmatrix} j_t & 1 & j_\mu \\ m_t & \mu & -m_\mu \end{pmatrix} v_{\kappa t \kappa \mu}, \quad (8)$$

where the radial hyperfine integral

$$c_{t\kappa\mu} = \int_0^\infty (g_{\kappa t}^* f_{\kappa\mu} + f_{\kappa t}^* g_{\kappa\mu}) dr, \quad (9)$$

and g being the radial functions of the small and large components, respectively. The relativistic quantum number

$$= -l - 1 \text{ for } j = l + \frac{1}{2} \text{ and } \kappa = l \text{ for } j = l - \frac{1}{2}.$$

Thus, for an s -state, $\kappa = -1$. The single expression 7 yields at the non-relativistic limit all second-order Ramsey terms $K^{(1b)}$, $K^{(2)}$ and $K^{(3)}$. At the non-relativistic limit the hyperfine integral v_{-1} is related to the spin density as

$$v_{-1} \equiv v_{-1-1} = -(2\pi/c) |\psi(0)|^2. \quad (10)$$

For heavier elements this formula cannot be used, the electron density at the nucleus (observable as Mössbauer isomer shifts) suffering much larger relativistic corrections than the hyperfine integral (for Sn, factors of about 2.31 and 35, respectively). Thus comparison of isomer shifts ($|\psi(0)|^2$) and spin—spin

coupling (ν_{-1}) [19] is in principle a questionable procedure, although a proportionality for a given element may still exist. We also remind the reader that the relativistic corrections for an element like Pb being 2.6, non-relativistic atomic $|\psi(\mathbf{C})|^2$ values [20a] are quite useless. The use of relativistic $|\psi(0)|^2$ instead of (9) [20b] is blatantly unphysical. Even for heavy-element compounds, a “contact part” can still be separated as one involving ν_{-1} or the s AOs on both nuclei.

Unless otherwise stated, the REX and EHT default parameters in the QCPE program [13] and the hyperfine integrals in ref. 1 are used in the present work.

2.3. How credible are the present results?

Following a suggestion by referees we should emphasize that we present this approach for the general reader as an exploratory one that should neither be blindly believed nor neglected. The most astute way of using rough theoretical methods like EHT or its counterpart REX, is as visual aids in finding explanations, such as symmetry rules, which must be there but which cannot be otherwise seen. Earlier examples of the use of such REX NMR results are the relation of the relativistic increase of the relative anisotropy, R , of the K tensor to a phase factor of $p_{1/2}$ AOs (ref. (1), § 4.2) and the discovery of the new symmetry rules for K [21b].

The dominant relativistic effects on heavy element chemistry, like the relativistic contraction of the 6s valence AOs, are now well established [16–18]. They are neither especially sophisticated nor small. To put it provocatively, it is better to do EHT including this contraction in the AOs, the energies and especially the hyperfine integrals, than to do ab initio calculations without it. In this light, the relativistic increase of the hyperfine integrals (especially ν_{-1} and ν_1) is definitely there, while the isolation of the Pb 6s AOs in deeper MOs (conclusion (d) below) is very plausible. The attribution of the observed strong changes of K to a node in a frontier MO, the HOMO (conclusion (c) below), is neither self-evident nor unreasonable and depends on the actual calculations performed. Confirming or disproving it theoretically will certainly take some time.

A remote analogy to this Pb 6s character in the HOMO of Pb_2Me_6 etc. is provided by the well-confirmed U 6p character in the HOMO of $U(\text{VI})$ compounds [14]. Finally we note that, because the s contribution dominates, a non-relativistic EHT formalism could have been used.

More technically speaking, the REX NMR model is non-iterative, thus exaggerating the charge transfer in heteropolar bonds. It gives a very limited set of virtual MOs (see, however, § 4.3 of ref. 1). It does not include any correlation effects, known to be important for spin–spin coupling (see ref. 9c). As to non-contact terms, the REX NMR ones are comparable to others for the $^1K(\text{CC})$ of C_2H_n ($n = 2, 4, 6$) (see Table 19 of ref. 9c) while they are much too small for HCl (see Table 8 of ref. 9c). Nevertheless, much insight to the experimental data has been obtained earlier at comparable level of theoretical sophistication.

Results

3.1. The model system $\text{HC}\equiv\text{CPbH}_3$

In order to study the sensitivity of the $^1K(\text{PbC})$ in $\text{R}_3\text{PbC}\equiv\text{CH}$ to the various

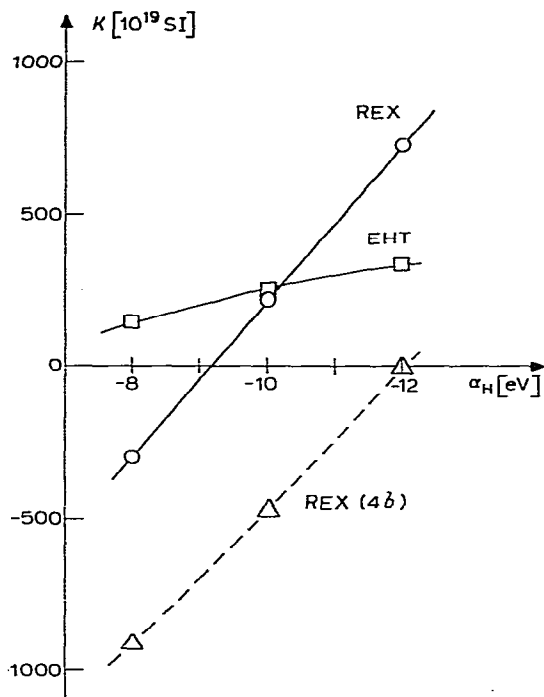


Fig. 1. Relativistic (REX) and non-relativistic (EHT) ${}^1K(\text{PbC})$ spin-spin coupling constants in $\text{HC}\equiv\text{CPbH}_3$ as a function of the hydrogen energy parameter α_H . For the REX case, the contribution from the highest occupied σ MO (4σ) is also shown.

substituents R [8], we first consider the model system $\text{H}_3\text{PbC}\equiv\text{CH}$, varying the electronegativity α_H of the hydrogens. The results are shown in Fig. 1. The REX K -value is indeed more sensitive than the EHT value to changes in α_H , passing through zero around $\alpha_H = -9$ eV. Secondly, both the ${}^1K(\text{PbC})$ and its variations are governed by the "contact-like" s -orbital contribution. Thirdly, although the contributions from the lower σ MOs are not negligible, the variation of $K(\text{REX})$ as a function of α_H is reproduced by the excitations from one MO only, namely the highest occupied σ MO, 4σ (summing over all j in eq. 2). The variations of $K(\text{EHT})$ are not governed by excitations from a single MO. Fourthly, the vanishing of this, negative contribution around $\alpha_H = -12$ eV can be attributed to a vanishing Pb $6s$ AO coefficient for this $6s(\text{Pb})$ – $2s(\text{C})$ anti-bonding 4σ MO.

The orbital energies of the free atoms and of HC_2PbH_3 are shown in Fig. 2. The α_{1s} passes α_{2p} at -11 eV. Then it is logical that the node plane near the Pb atom could pass exactly through it, giving a zero $6s$ coefficient, if the group of three $1s$ AOs on the right-hand side have the same electronegativity as the carbon $2p$ AO on the left hand side of the Pb atom.

Summarizing, the sensitivity of the ${}^1K(\text{PbC})$ would thus be due first to the relativistic stabilization of the 2σ and 3σ MOs, making their contribution a constant one, and second to a node plane near the lead nucleus for the 4σ MO.

One also sees from Fig. 2 that, around $\alpha_H = -12$ eV, the 4σ and 2π ($\frac{1}{2}$) MOs

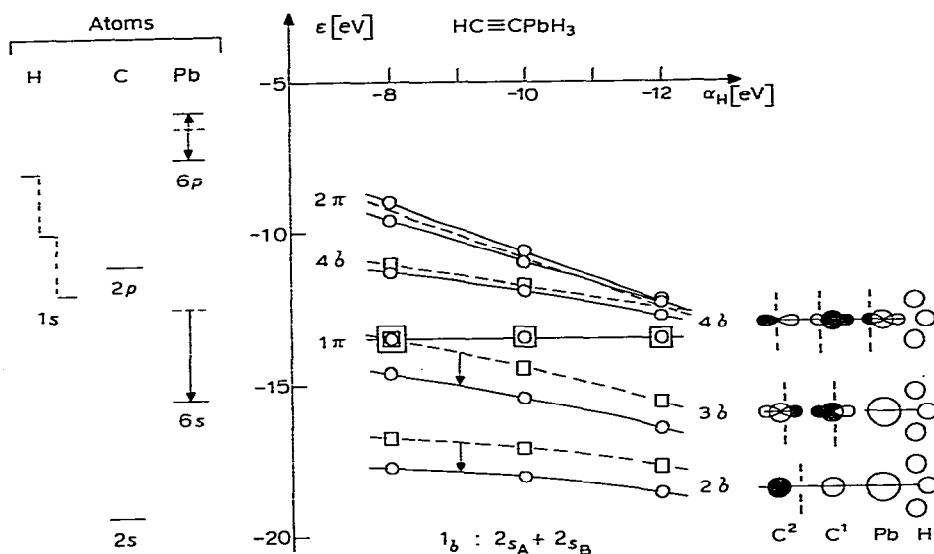


Fig. 2. The REX (full lines and circles) and EHT (dashed lines and squares) MO energies of $\text{HC}\equiv\text{CPbH}_3$ as a function of α_{H} . The relativistic stabilization is indicated by arrows. Note the avoided crossing of the 4σ and $2\pi(\bar{2})$ (lower 2π) curves around $\alpha_{\text{H}} = -12$ eV.

have an avoided crossing. Then it is logical that the $6s$ character should vanish; in a tetrahedrally symmetric surrounding the Pb p orbitals span a two-fold degenerate $\Gamma_7(e_{5/2})$ MO and a four-fold degenerate $\Gamma_8(g_{1/2})$ MO only. The Pb $6s$ then belongs to the $\Gamma_6(e_{1/2})$ MO, not represented. Another way of studying the sensitivity of ${}^1K(\text{PbC})$ to small perturbations, is to change the acetyl hydrogen ζ from 1.2 to 1.0. This increases $K(\text{EHT})$ by 3 (10^{19} SI) only but $K(\text{REX})$ by 17 (at $\alpha_{\text{H}} = -10$). Changing, furthermore, Pb—C from 2.19 to 2.10 Å increases by 54 and 225, for EHT and REX, respectively.

The local symmetry of the Pb—H bond is C_s . For this symmetry, if $\sigma(xy)$ is the symmetry plane, the antisymmetric components $K^{(a)}(xz)$ and $K^{(a)}(yz)$ may be non-zero [21]. With the present method, EHT gives no such $K^{(a)}$ (PbH) while REX gives (at $\alpha_{\text{H}} = -8$) an antisymmetric component of the order of 100 (10^{19} SI).

The isotropic $K(\text{PbH})$ of about 900 is quite insensitive to the changes discussed above; the experimental value in PbHMe_3 is 938. For ${}^1K(\text{PbH})$ the contributions from the 2σ and 3σ MOs are of the same sign while for ${}^1K(\text{PbC})$ they were of opposite sign (see Fig. 2). Therefore the 4σ contribution is less important, which explains this insensitivity.

Sebald and Wrackmeyer [27] observed that the values of ${}^1K(\text{C}\equiv\text{C})$ in the $\text{R}_3\text{Pb}-\text{C}\equiv\text{C}-\text{R}'$ compounds are only about 70% of that in acetylene. Attempts to reproduce this tendency by the present method were not successful.

3.2. The tetrahedral system $M(\text{CCH})_4$, $M = \text{Sn}, \text{Pb}$: the role of radial nodes

In these molecules we have six totally symmetric (a_1) MOs, spanned by the $6s$, $2s_1$, $2p\sigma_1$, $2s_2$, $2p\sigma_2$ and $1s$ AOs. The three lowest of them are occupied. The ${}^1K(\text{PbC})$ coupling constants in Tab. 1 still are mainly contact, i.e. proportional to the product $c_i(6s)c_i(2s_1)c_j(6s)c_j(2s_1)/(E_i - E_j)$, i being the occupied

TABLE 1

CALCULATED AND OBSERVED SPIN-SPIN COUPLING CONSTANTS ${}^1K(\text{MC})$ AND THEIR RELATIVE ANISOTROPIES $R = (K_{\parallel} - K_{\perp})/K$

Molecule	${}^1K(\text{MC})$			$R(\text{MC})$	
	EHT	REX	Exp ^a	EHT	REX
Sn(CCH) ₄	212	289	1032	0.527	0.586
Pb(CCH) ₄	336	837	2547	0.527	0.794

^a Ref. 8.

and j the empty MO. In contrast to the simple cases "without s -hybridized lone pairs" in ref. 1, we now have, in addition to the Pb-C¹ bonding $1a_1$ and $2a_1$ MO:s the third occupied $3a_1$ MO which is $6s-2s_1$ anti-bonding, giving a negative ${}^1K(\text{Pb-C})$ contribution. Among the empty MOs, the excitations to the antibonding $j = 4a_1$ MO dominate. E.g. in the $M = \text{Pb}$, REX case the $1a_1 \rightarrow 4a_1$, $2a_1 \rightarrow 4a_1$, and $3a_1 \rightarrow 4a_1$ contributions to ${}^1K(\text{PbC})$ are 557, 1174 and -693×10^{19} SI, respectively.

The existence of these cancellation effects may explain why the calculated ${}^1K(\text{MC})$ in Tab. 1 are much smaller than experimental values. The ratio $K(\text{PbC})/K(\text{SnC})$ is 1.58, 2.89 and 2.47 according to EHT, REX, and experimental values, respectively. As seen from Table 2, the relativistic Pb case again is much more sensitive to small perturbations, such as changing the peripheral ξ_{H} from 1.0 to 1.2 or lowering the Pb atomic energy levels by 2 eV. As stated in Table 2, the

TABLE 2

EFFECT OF THE CHANGES $\xi_{\text{H}} = 1.0 \rightarrow 1.2$ and $\alpha_{\text{Pb}} \rightarrow \alpha_{\text{Pb}} - 2 \text{ eV}$ ON THE CALCULATED ${}^1K(\text{MC})$ IN $\text{M}(\text{CCH})_4$.

Case	M = Sn		M = Pb	
	EHT	REX	EHT	REX
A	212	289	336	837
B	218	299	346	876
$\Delta(B - A)$	6	9	10	38
C	—	—	344	748
$\Delta(C - B)$	—	—	-2	-128 ^a

A = default parameters. B: $\xi_{\text{H}} = 1.2$. C: $\xi_{\text{H}} = 1.2$, all Pb levels decreased by 2 eV.

^a Contribution from $3a_1 \rightarrow 4a_1$ only: -129.

TABLE 3

EXPERIMENTAL ${}^1K(\text{MC})$ COUPLING CONSTANTS IN MR_4 MOLECULES (IN 10^{19} SI).

M	R		Decrease
	CH ₃	CH ₃ CH ₂	
Sn ^a	298	283	15
Pb ^b	392	318	74

^a Ref. 22. ^b Ref. 23.

sensitivity may again be attributed to the a_1 HOMO—LUMO or $3a_1 \rightarrow 4a_1$ contribution, and more particularly to a node plane, now near the carbon, giving a very small $c_{3a_1}(2s)$.

It is interesting to observe that for PbR_4 , the change of ${}^1K(\text{MC})$ from $\text{R} = \text{Me}$ to $\text{R} = \text{Et}$ in Table 3 is much larger than for SnR_4 .

3.3. The model system Pb_2H_6

In ref. 1, with the default parameters of the program, we were unable to reproduce the small, observed ${}^1K(\text{PbPb})$ in Pb_2Me_6 . As the simplest possible test system we now first consider Pb_2H_6 , varying again α_{H} to simulate the various ligands.

The calculated ${}^1K(\text{PbPb})$ coupling constant as a function of α_{H} is shown in Fig. 3. The filled σ MOs are also sketched. The coupling is again predominantly contact. The sum of the large but opposite $1\sigma_{\text{g}}$ and $1\sigma_{\text{u}}$ contributions is again small and nearly constant. The variations of the total $K(\text{PbPb})$ are largely explained by the $2\sigma_{\text{g}}$ contribution, whose 6s character approaches zero around $\alpha_{\text{H}} = -8$ eV. Thus, due to the relativistic stabilization of the 6s AO, the $1\sigma_{\text{g}}$ and $1\sigma_{\text{u}}$ contributions largely cancel and the $2\sigma_{\text{g}}$ contribution vanishes if a node plane traverses the Pb nucleus.

As seen from Fig. 3, both the $1\sigma_{\text{g}}$ and the $1\sigma_{\text{u}}$ are Pb—H bonding. Thus their contributions to ${}^1K(\text{PbH})$ are of the same sign and dominate the total value which, consequently, is rather insensitive to α_{H} (592 , 653 and 618×10^{19} SI for an α_{H} of -8 , -10 and -12 eV, respectively).

3.4. Hexamethyl diplumbane

The calculated ${}^1K(\text{PbPb})$ and ${}^1K(\text{PbC})$ coupling constants are shown in Fig. 4. Because the default parameters in the REX program exaggerate the charge transfer from lead to the methyl groups, we experiment by lowering the Pb 6s and 6p levels by a few eV. This diminishes the Mulliken charge $Q(\text{Pb})$, as shown in Fig. 4. Perhaps the most interesting conclusion is that even for Pb_2Me_6 , with 50 valence electrons, the excitations from the σ HOMO (MOs 49–50)

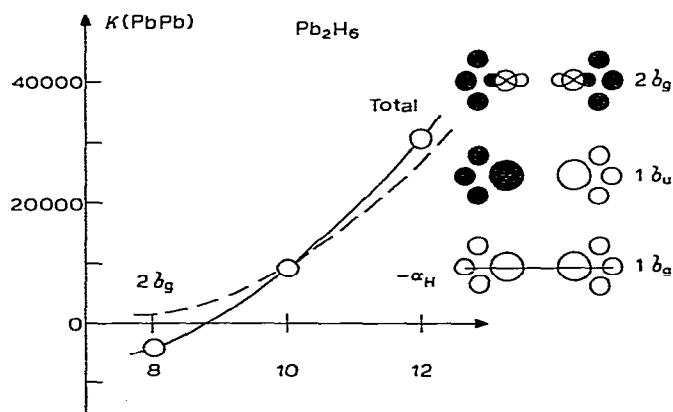


Fig. 3. The REX ${}^1K(\text{PbPb})$ (in 10^{19} SI) as a function of α_{H} . The contribution from the $2\sigma_{\text{g}}$ HOMO only is also shown.

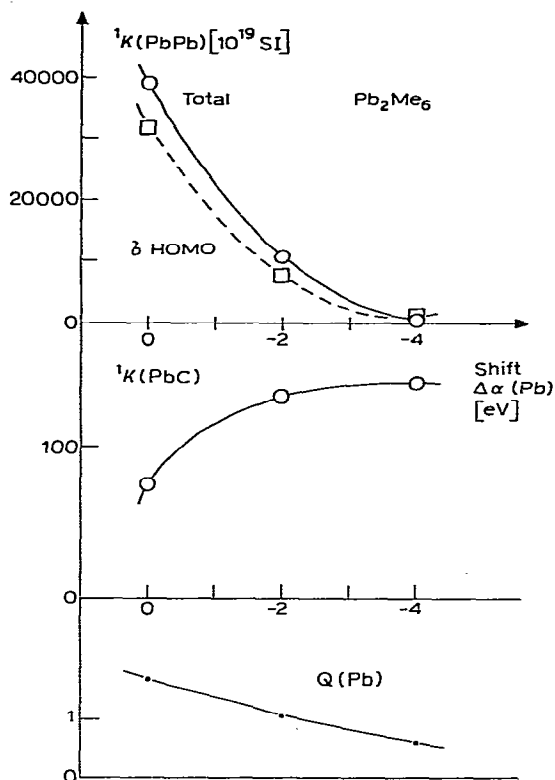


Fig. 4. The ${}^1K(\text{PbPb})$ and ${}^1K(\text{PbC})$ coupling constants and the Mulliken charge on the Pb atom in $\text{Pb}_2(\text{CH}_3)_6$ as a function of the shift of the Pb levels from $\alpha_{6s} = -15.416$, $\alpha_{6p_{1/2}} = -7.486$ and $\alpha_{6p_{3/2}} = -5.984$ eV.

alone suffice to explain the variations of ${}^1K(\text{PbPb})$ as a function of $\alpha(\text{Pb})$. When the Pb level shift $\Delta\alpha(\text{Pb})$ is around -4 eV, ${}^1K(\text{PbPb})$ approaches zero, because of a vanishing $6s$ coefficient. The experimental ${}^1K(\text{PbPb})$ is 553×10^{19} SI [3,6]. The experimental ${}^1K(\text{PbC})$ is 44×10^{19} SI [7], compared to the values of 392 in PbMe_4 or 318 in PbEt_4 in Table 3. No dominant single contribution to the ${}^1K(\text{PbC})$ was found. Anyway, the sum (Fig. 4) of the various, largely cancelling contributions to ${}^1K(\text{PbC})$ is small, although a simple explanation cannot be offered.

The orbital energies of Pb_2Me_6 are shown in Fig. 5. Due to the relativistic stabilization (from EHT to REX) of the Pb $6s$ levels, they are predicted to form two separate levels (σ_g and σ_u) below the $\text{C}(2p) + \text{H}(1s)$ band of the methyls. As shown in Fig. 4 (difference between the σ HOMO and total contributions), the individually large σ_g and σ_u contributions largely cancel. The behaviour of the observed ${}^1K(\text{PbPb})$ is determined by the σ HOMO contribution, which vanishes due to a vanishing $6s$ coefficient around $\Delta\alpha(\text{Pb}) = -4$ eV. It would be very interesting to have the photoelectron spectrum of Pb_2Me_6 to check Fig. 5. Such spectra were reported for M_2Me_6 ($\text{M} = \text{C-Sn}$) by Szepes et al. [26]. We predict that a Pb $6s$ band should appear around 18–19 eV for Pb_2Me_6 .

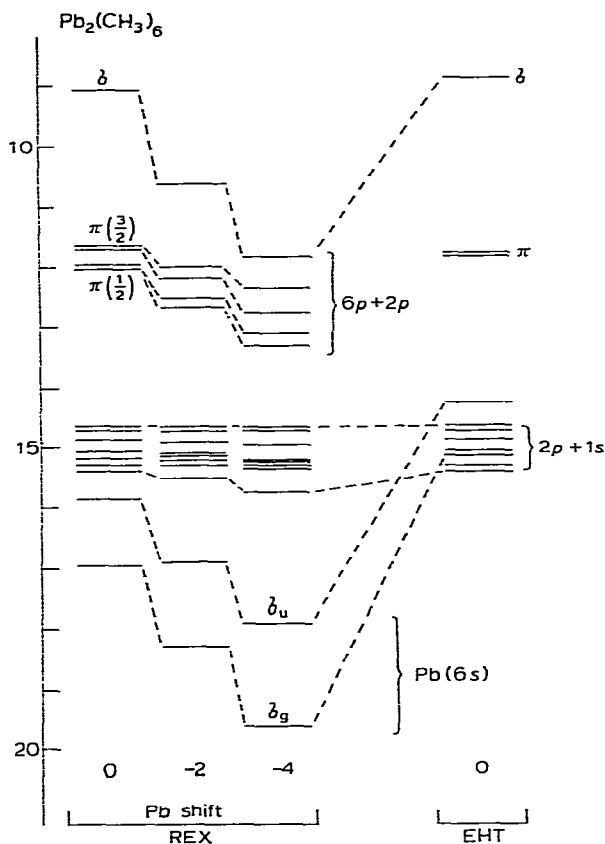


Fig. 5. The orbital energies of Pb_2Me_6 .

Both these photoelectron spectra and the radical cation EPR spectra [24] suggest a metal-metal σ -bonding HOMO.

4. Technical details

All hyperfine integrals were taken from ref. 1. The default parameters of the program [13–14] were used unless otherwise stated. The $4d$ AOs of Sn and $5d$ AOs of Pb were omitted. The other parameters used were as follows: HC_2PbH_3 : Pb–C: 2.19, C–C: 1.20, C–H: 1.06, Pb–H: 1.748 Å, $\zeta_{\text{H}} = 1.20$. $\text{M}(\text{CCH})_4$: Sn–C: 2.14 Å, $\zeta_{\text{H}} = 1.0$, $\alpha_{\text{H}} = -13.6$ eV, otherwise as above. Pb_2H_6 : Pb–Pb: 2.88, Pb–H: 1.748 Å, $\zeta_{\text{H}} = 1.20$. $\text{Pb}_2(\text{CH}_3)_6$: Pb–Pb: 2.88, Pb–C: 2.25, C–H: 1.09 Å, all angles tetrahedral. Default hydrogen ($\zeta_{\text{H}} = 1.0$, $\alpha_{\text{H}} = -13.6$).

5. Conclusions

With due reservations for the approximate MO model used, the following conclusions are found: (a) The isotropic coupling constants discussed are mainly “contact”, i.e. involve s AOs on both nuclei. The non-contact parts

are important only for the anisotropic part of the K tensor.

(b) We fully agree with the earlier expectations [3,5,8,19,20b,25] that the large variations in ${}^1K(\text{MM})$ and ${}^1K(\text{MC})$ are due to the mutual polarisability π , eq. 2.

(c) More specifically, the negative ${}^1K(\text{PbC})$ in some $\text{R}_3\text{PbC}\equiv$ systems and the small ${}^1K(\text{PbPb})$ in Pb_2Me_6 are attributed to a node near the Pb nucleus in the highest occupied σ MO, whose variations mainly determine the variations of the total K . Thus the sensitivity of these coupling constants to substituents is a frontier-orbital effect.

(d) Due to the relativistic stabilization of the Pb 6s shell, most of the 6s character resides in deeper MOs. Contributions from them to spin-spin coupling do not necessarily vanish, but are less sensitive to substitution.

Acknowledgement

I wish to thank Drs. J. Kowalewski and B. Wrackmeyer for reading the manuscript.

References

- 1 P. Pyykkö and L. Wiesenfeld, *Mol. Phys.*, **43** (1981) 557.
- 2 T.N. Mitchell, J. Gmehling and F. Huber, *J. Chem. Soc., Dalton Trans.*, (1978) 960.
- 3 J.D. Kennedy, W. McFarlane and B. Wrackmeyer, *Inorg. Chem.*, **15** (1976) 1299.
- 4 T.N. Mitchell, *J. Organometal. Chem.*, **70** (1974) C1.
- 5 J.D. Kennedy and W. McFarlane, *J. Chem. Soc., Chem. Comm.*, (1974) 983; *J. Chem. Soc., Dalton Trans.*, (1976) 1219.
- 6 R.J.H. Clark, A.G. Davies, R.J. Puddephatt and W. McFarlane, *J. Amer. Chem. Soc.*, **91** (1969) 1334.
- 7 J.D. Kennedy and W. McFarlane, *J. Organometal. Chem.*, **80** (1974) C47.
- 8 B. Wrackmeyer, *J. Magn. Reson.*, **42** (1981) 287.
- 9 (a) N.F. Ramsey, *Phys. Rev.*, **91** (1953) 303; (b) J.A. Pople and D.P. Santry, *Mol. Phys.*, **8** (1964) 1; (c) J. Kowalewski, *Ann. Rep. NMR Spectr.*, in press.
- 10 T. Birchall and A. Pereira, *J. Chem. Soc., Chem. Comm.*, (1972) 1150.
- 11 P. Pyykkö, *Chem. Phys.*, **22** (1977) 289.
- 12 L.L. Lohr Jr. and P. Pyykkö, *Chem. Phys. Letters*, **62** (1979) 333.
- 13 L.L. Lohr Jr., M. Hotokka and P. Pyykkö, *Quantum Chem. Progr. Exchange*, **12** (1980) 387.
- 14 P. Pyykkö and L.L. Lohr, Jr., *Inorg. Chem.*, **20** (1981) 1950.
- 15 L.L. Lohr Jr., *Inorg. Chem.*, **20** (1981) 4229.
- 16 P. Pyykkö, *Adv. Quantum Chem.*, **11** (1978) 353.
- 17 K.S. Pitzer, *Accounts Chem. Res.*, **12** (1979) 271.
- 18 P. Pyykkö and J.P. Desclaux, *Accounts Chem. Res.*, **12** (1979) 276; *C.R. Acad. Sci.*, (Paris), **292** (1981) 1513.
- 19 T.N. Mitchell and M. el-Beahiry, *Helv. Chim. Acta*, **64** (1981) 628.
- 20 (a) P.S. Pregosin and R.W. Kunz, *NMR Basic Principles and Progress*, Vol. 16, Ed. P. Diehl, Springer, Berlin 1979; (b) R.W. Kunz, *Helv. Chim. Acta*, **63** (1980) 2054.
- 21 (a) A.D. Buckingham and I. Love, *J. Magn. Reson.*, **2** (1970) 338. (b) A.D. Buckingham, P. Pyykkö, J.B. Robert and L. Wiesenfeld, *Mol. Phys.*, in press.
- 22 H.G. Kuivila, J.L. Considine, R.H. Sharma and R.J. Mynott, *J. Organometal. Chem.*, **111** (1976) 179.
- 23 R.H. Cox, *J. Magn. Reson.*, **33** (1979) 61.
- 24 J.T. Wang and F. Williams, *J. Chem. Soc., Chem. Comm.*, (1981) 666.
- 25 T. Iwayanagi and Y. Saito, *Chem. Letters (Japan)*, (1976) 1193.
- 26 L. Szepes, T. Korányi, G. Náráay-Szabó, A. Modelli and G. Distefano, *J. Organometal. Chem.*, **217** (1981) 35.
- 27 A. Sebald and B. Wrackmeyer, *Spectrochim. Acta*, **37A** (1981) 365.
- 28 M.C.R. Symons, *J. Chem. Soc., Chem. Commun.*, (1981) 1251.

Note added in proof: Symons [28] recently reported for Me_6Sn_2^+ an Sn 5s orbital population of about 1% from ESR spectra. In agreement with this, our Pb_2Me_6 HOMO has a 6s population of 4, 1 and 0.2% and a 6p population of 30, 28 and 21% at the shifts, $\Delta\alpha$, of 0, -2 and -4 eV, respectively. Symons deduces for Me_6Sn_2^+ a 5p population of 35%.

For Ph_6Sn_2^- , a large 5s hyperfine coupling was obtained. The present Pb_2Me_6 LUMO indeed shows a 6s population of 18, 6 or 2% at the $\Delta\alpha$ values, mentioned above.